

Vibration attenuation in periodic composite Timoshenko beams on Pasternak foundation

Hong-Jun Xiang* and Zhi-Fei Shi^a

School of Civil Engineering, Beijing Jiaotong University, Beijing 100044, China

(Received December 8, 2010, Revised June 30, 2011, Accepted August 17, 2011)

Abstract. Periodic and quasi-periodic Timoshenko beams on Pasternak foundation are investigated using the differential quadrature method. Not only band gaps in the beams but also the dynamic response of them is analyzed. Numerical results show that vibration in periodic beams can be dramatically attenuated when the exciting frequency falls into band gaps. Different from the band structures of periodic beams without foundation, the so-called critical frequency was found because of the Pasternak foundation. Its physical meaning was explained in detail and a useful formula was given to calculate the critical frequency. Additionally, a comprehensive parameter study is conducted to highlight the influence of foundation modulus on the band gaps.

Keywords: vibration attenuation; periodic beams; band gap; dynamic response; Pasternak foundation

1. Introduction

The propagation of elastic waves in composite materials or structures with periodic material properties or periodic geometrical shapes has received considerable attention in recent years. These materials or structures are called periodic materials or structures. By nature, they exhibit unique dynamic characteristics that make them act as mechanical filters for wave propagation in a special frequency range called 'band gaps'. Recently, inspired by the band gap of periodic structures, Jia and Shi (2010) fabricated a finite quasi-periodic foundation to reduce the effect of earthquake waves on structures. It is found that 1) frequency band gap also exists in the periodic foundation; 2) the foundation can be fabricated to realize a low frequency gap which can be smaller than 20 Hz. Therefore, the periodic foundation lends a new insight into seismic isolation in civil engineering.

A lot of works have been done on periodic materials or structures. An extensive review of the earlier research in periodic structures can be found by Mead (1996). The theory of periodic structures was originally developed for solid state applications and extended, in the early seventies, to the design of mechanical structures. Since then, the theory has been applied extensively to a wide variety of structures such as spring-mass systems (Faulkner and Hong 1985), periodically supported beams (Lin *et al.* 1990), stiffened plates (Mead 1986), cylindrical shells (Pany *et al.* 2003) and lattice structures (Fan *et al.* 2007). Most of these studies concerned structures with periodically

*Corresponding author, Associate Professor, E-mail: hjxiang@bjtu.edu.cn, xianghj@gmail.com

^aProfessor, E-mail: zfshi178@sohu.com

distributed geometrical characters such as shape or supports. On the other hand, Kushwaha *et al.* (1993) presented a novel concept of phononic crystals (PCs) of which the material properties are periodic distribution. Since then, analytical, numerical, and experimental studies have been conducted to analyze the band gap behavior of periodic materials (Kushwaha 1996).

As far as the analytical or numerical method is concerned, many methods have been proposed to determine the band gaps in periodic materials, such as the plane-wave expansion method (Yao *et al.* 2009), the multiple scattering theory (Sainidou *et al.* 2005), the finite difference time-domain method (Hsieh *et al.* 2006), the lumped mass method (Wang *et al.* 2004), and the finite element method (Khelif *et al.* 2006). Despite the benefits of them, these methods encounter some difficulties (Xiang and Shi 2009). For example, the PWE method encounters convergence problems when the periodic material has a large elastic mismatch; and the MST method has a limitation in studying periodic materials with overlap scatters. In recent years, the differential quadrature method (DQM) has been proven adequately proficient coupled with various beam or plate theories (Shu and Richards 1992, Bert and Malik 1996). Recently, Xiang and Shi (2009) first applied the DQM to the band gap analysis in periodic structures and shown that the method is very accurate and simple.

It is also noted that most of the previous studies dealt with band gaps in geometrical periodic structures or infinite periodic composite materials. Investigations on quasi-periodic composite structures are scarce. Moreover, other two important factors should be considered if we want to apply the concept of periodic structures in engineering. One is that engineering structures are finite dimensional, so further study on finite dimensional structures, such as plates and beams, is of importance. Another one is the soil-structure interaction (SSI) which is one of the structural engineering problems of theoretical and practical interest. In order to model soil behavior, several models have been developed in the past. Two important examples are the Winkler model and the Pasternak model. The Winkler model assumes the soil to be made up of continuously distributed, non-connected discrete springs. Thanks to its simplicity, a number of studies in the area of soil-structure interaction have been conducted. However, the soil represented by Winkler model cannot sustain shear stresses because of the discrete springs and hence no spread of load to parts of mass that are not directly loaded occur (Celep and Demir 2007, Coskun 2010). Its discontinuous nature gives rise to the development of the Pasternak model in which the existence of shear interaction among the spring elements is assumed by connecting the ends of the springs to a shear layer. The Pasternak model describes soil behavior more accurately and yet remains simple enough for practical purposes.

In consideration of the aspects above, different types of periodic or quasi-periodic composite Timoshenko beams on Pasternak foundations are fabricated in this work. We focus on the effect of the foundation on the band gaps and vibration attenuation in the beams. The organization of this paper is as follows. Based the Bloch-Floquet theorem (Kittel 2005), the Timoshenko beam theory is adopted to analyze the periodic beam in Section 2. In Section 3, the DQM is introduced to solve the dynamic equations of periodic beams. The accuracy and flexibility of the methods are validated in Section 4 by way of comparison to existing solutions available in previous studies of homogeneous beams. In Section 5, the band gaps in the beams, the harmonic frequency response and the transient response of the beams are studied. Additionally, a comprehensive parameter study is conducted to highlight the effect of elastic foundation on band gaps in periodic beams. Finally, Section 6 provides a short conclusion.

2. Timoshenko periodic beam theory

A periodic composite beam consisting of alternating beam sections A and B of lengths a_1 and a_2 , respectively, is shown in Fig. 1(a).

2.1 Basic equations

The entire beam is divided into N_e elements based on the discontinuities in geometry, boundary constraints and materials properties. Each element is an isotropic uniform beam section. The length of the element n is equal to l_n as shown in Fig. 1(b). Based on the Timoshenko beam theory, for a given element of the periodic beam on a Pasternak foundation, the equation of motion can be written as follows (Wang *et al.* 1998)

$$E^{(n)}I^{(n)}\frac{\partial^2\psi^{(n)}}{\partial x^2} + k_s^{(n)}G^{(n)}A^{(n)}\left(\frac{\partial w^{(n)}}{\partial x} - \psi^{(n)}\right) = \rho^{(n)}I^{(n)}\frac{\partial^2\psi^{(n)}}{\partial t^2} \tag{1}$$

$$k_s^{(n)}G^{(n)}A^{(n)}\left(\frac{\partial^2 w^{(n)}}{\partial x^2} - \frac{\partial \psi^{(n)}}{\partial x}\right) - K_w^{(n)}w^{(n)} + K_G^{(n)}\frac{\partial^2 w^{(n)}}{\partial x^2} + q = \rho^{(n)}A^{(n)}\frac{\partial^2 w^{(n)}}{\partial t^2} \tag{2}$$

where E is the Young’s Modulus, G the Shear modulus, A the cross-section area, ρ the beam density, I the second area moment of inertia about the neutral axis, K_w the Winkler foundation modulus, K_G the shear foundation modulus, k_s the shear correction factor ($k_s = 5/6$ for rectangle cross-section), w the transverse deflection, ψ the bending slope, t the time and x the local coordinate

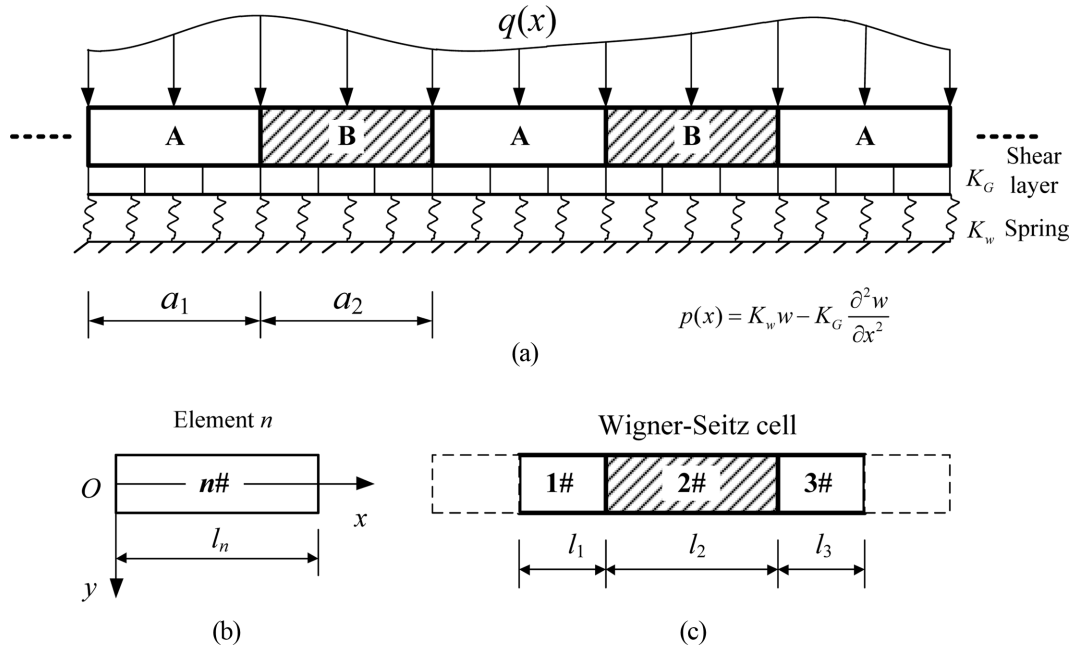


Fig. 1 Configuration of a periodic composite beam on elastic foundation (a) composite beam consisting of an infinite repetition of alternating sections A and B, (b) one element, and (c) Wigner-Seitz cell

($x \in [0, l_n]$), respectively. The superscript (n) indicates the n -th element. The moment M and the generalized shear force Q are

$$M^{(n)} = -E^{(n)} I^{(n)} \frac{\partial \psi^{(n)}}{\partial x}, \quad Q^{(n)} = k_s^{(n)} G^{(n)} A^{(n)} \left(\frac{\partial w^{(n)}}{\partial x} - \psi^{(n)} \right) + K_G \frac{\partial w}{\partial x} \quad (3)$$

The second term in the shear force Q is the contribution from foundation (Zhaohua and Cook 1983). The compatibility of deflection, slope, moment and shear force at the junction of two adjacent elements ' n ' and ' $n+1$ ' can be expressed as

$$\begin{aligned} w^{(n)} \Big|_{x=l_n} &= w^{(n+1)} \Big|_{x=0}, \quad \psi^{(n)} \Big|_{x=l_n} = \psi^{(n+1)} \Big|_{x=0} \\ M^{(n)} \Big|_{x=l_n} &= M^{(n+1)} \Big|_{x=0}, \quad Q^{(n)} \Big|_{x=l_n} = Q^{(n+1)} \Big|_{x=0} \end{aligned} \quad (4)$$

An infinite periodic beam may be created as a regular repetition of a substructure in space. Therefore, the infinite periodic beam can be simplified to a unit substructure (or cell) using Bloch-Floquet theorem (Kittel 2005) as shown in Fig. 1(c). Herein, the well-known Wigner-Seitz cell (Kittel 2005) containing three elements ($N_e = 3$) with length l_1, l_2, l_3 ($l_1 = l_3 = a_1/2$ and $l_2 = a_2$) will be adopted in the present paper. According to Bloch-Floquet theorem, the deflection, slope, moment and shear force obey a periodic law (Yu *et al.* 2008, Xiang and Shi 2009) as follows

$$\begin{aligned} w^{(3)} \Big|_{x=l_3} &= e^{ik_x a} w^{(1)} \Big|_{x=0}, \quad \psi^{(3)} \Big|_{x=l_3} = e^{ik_x a} \psi^{(1)} \Big|_{x=0} \\ M^{(3)} \Big|_{x=l_3} &= e^{ik_x a} M^{(1)} \Big|_{x=0}, \quad Q^{(3)} \Big|_{x=l_3} = e^{ik_x a} Q^{(1)} \Big|_{x=0} \end{aligned} \quad (5)$$

where k_x is a Floquet wave number in the x direction (Lee and Ke 1992), which counts the number of wavelength over 2π distance, and a is the length of the cell $a = a_1 + a_2$. Eq. (5) contain four boundary conditions for an infinite periodic beam. Eqs. (1)-(5) can be considered as a typical boundary value problem.

The structure itself may be finite, i.e., at the both ends usual boundary conditions can be applied. To model the finite quasi-periodic beam, the four periodic boundary conditions (5) should be replaced by its specific boundary conditions. The beam may be simply supported (S), clamped (C) or free (F) at its ends. If the boundary element of the beam is numbered as m , for example, the boundary conditions are expressed as follows

$$\text{Simply supported (S):} \quad w^{(m)} = w_0, \quad M^{(m)} = M_0 \quad (6)$$

$$\text{Clamped (C):} \quad w^{(m)} = w_0, \quad \psi^{(m)} = \psi_0 \quad (7)$$

$$\text{Free (F):} \quad Q^{(m)} = Q_0, \quad M^{(m)} = M_0 \quad (8)$$

where w_0, ψ_0, M_0, Q_0 are the given displacement, rotation, moment and shear force, respectively, at the boundary. Each end has two boundary conditions. Thus there are four boundary conditions for a finite quasi-periodic beam. Eqs. (1)-(4) together with these four conditions represent another boundary value problem.

The DQM will be adopted to solve above mentioned two types of boundary value problems. In

order to apply the DQM conveniently and to avoid a singular coefficient matrix involved in DQM, i.e., to get a robust numerical result, all equations should be normalized.

2.2 Dimensionless form of the basic equations

By introducing the following dimensionless quantities

$$\eta = \frac{x}{l_i}, \quad v^{(n)} = \frac{w^{(n)}}{l_0}, \quad \tau = t \sqrt{\frac{E_0}{\rho_0 A_0}}, \quad \bar{Q}^{(n)} = \frac{Q^{(n)}}{G_0 A_0}, \quad \bar{M}^{(n)} = \frac{M^{(n)} l_0}{E_0 I_0} \tag{9}$$

where $l_0, E_0, G_0, A_0, I_0, \rho_0$ are the reference length, modulus of elasticity, modulus of rigidity, cross-section area, second area moment of inertia, density of a specific element, the governing Eq. (1)-(2) can be expressed in dimensionless form as

$$\alpha_{1n} \frac{\partial v^{(n)}}{\partial \eta} + \alpha_{2n} \psi^{(n)} + \alpha_{3n} \frac{\partial^2 \psi^{(n)}}{\partial \eta^2} + \frac{\partial^2 \psi^{(n)}}{\partial \tau^2} = 0 \tag{10}$$

$$\beta_{1n} v^{(n)} + \beta_{2n} \frac{\partial^2 v^{(n)}}{\partial \eta^2} + \beta_{3n} \frac{\partial \psi^{(n)}}{\partial \eta} + \frac{\partial^2 v^{(n)}}{\partial \tau^2} = f^{(n)} \tag{11}$$

where $f^{(n)} = \rho_0 A_0 q / \rho^{(n)} A^{(n)} l_0 E_0$ and the dimensionless quantities α_{ij} and β_{ij} are listed in Appendix A. With Eq. (3) in mind, the continuous Eq. (4) can be rewritten as

$$v^{(n)} \Big|_{\eta=1} = v^{(n+1)} \Big|_{\eta=0} \tag{12}$$

$$\psi^{(n)} \Big|_{\eta=1} = \psi^{(n+1)} \Big|_{\eta=0} \tag{13}$$

$$\gamma_{1n} \frac{\partial \psi^{(n)}}{\partial \eta} \Big|_{\eta=1} = \gamma_{1,n+1} \frac{\partial \psi^{(n+1)}}{\partial \eta} \Big|_{\eta=0} \tag{14}$$

$$\left(\gamma_{2n} \psi^{(n)} + \gamma_{3n} \frac{\partial v^{(n)}}{\partial \eta} \right) \Big|_{\eta=1} = \left(\gamma_{2,n+1} \psi^{(n+1)} + \gamma_{3,n+1} \frac{\partial v^{(n+1)}}{\partial \eta} \right) \Big|_{\eta=0} \tag{15}$$

and the periodic boundary conditions (5) are rewritten as

$$v^{(3)} \Big|_{\eta=1} = e^{ik\pi} v^{(1)} \Big|_{\eta=0} \tag{16}$$

$$\psi^{(3)} \Big|_{\eta=1} = e^{ik\pi} \psi^{(1)} \Big|_{\eta=0} \tag{17}$$

$$\gamma_{13} \frac{\partial \psi^{(3)}}{\partial \eta} \Big|_{\eta=1} = e^{ik\pi} \gamma_{11} \frac{\partial \psi^{(1)}}{\partial \eta} \Big|_{\eta=0} \tag{18}$$

$$\left(\gamma_{23} \psi^{(3)} + \gamma_{33} \frac{\partial v^{(3)}}{\partial \eta} \right) \Big|_{\eta=1} = e^{ik\pi} \left(\gamma_{21} \psi^{(1)} + \gamma_{31} \frac{\partial v^{(1)}}{\partial \eta} \right) \Big|_{\eta=0} \tag{19}$$

where $k = k_x a / \pi$ is the dimensionless wave number. Similarly, for a finite quasi-periodic beam, the dimensionless end support conditions can be rewritten as follows.

Simply supported (S)

$$v^{(m)} = v_0 \equiv w_0 / l_0, \gamma_{1m} \frac{\partial \psi^{(m)}}{\partial \eta} = \bar{M}_0 \quad (20)$$

Clamped (C)

$$v^{(m)} = v_0 \equiv w_0 / l_0, \psi^{(m)} = \psi_0 \quad (21)$$

Free (F)

$$\gamma_{2m} \psi^{(m)} + \gamma_{3m} \frac{\partial v^{(m)}}{\partial \eta} = \bar{Q}_0, \gamma_{1m} \frac{\partial \psi^{(m)}}{\partial \eta} = \bar{M}_0 \quad (22)$$

The dimensionless quantities γ_{ij} in Eqs. (14)-(22) are listed in Appendix A.

3. Solution method

The DQM is used to solve Eqs. (10), (11) and the associated continuous and boundary conditions. The fundamental idea behind the DQM is to approximate an unknown function and its derivative at any discrete point as the linear weighted sums of its values at all of the discrete points chosen in the solution domain. The functions $v^{(n)}(\eta)$, $\psi^{(n)}(\eta)$ and their r -th derivatives with respect to η are approximated by

$$\{v^{(n)}(\eta), \psi^{(n)}(\eta)\} = \sum_{j=1}^N l_j(\eta) \{v_j^{(n)}, \psi_j^{(n)}\} \quad (23)$$

$$\frac{\partial^r}{\partial \eta^r} \{v^{(n)}, \psi^{(n)}\} \Big|_{\eta=\eta_i} = \sum_{j=1}^N C_{ij}^{(r)} \{v_j^{(n)}, \psi_j^{(n)}\} \quad (24)$$

where $v_j^{(n)} = v^{(n)}(\eta_j)$, $\psi_j^{(n)} = \psi^{(n)}(\eta_j)$, N is the total number of nodes distributed along the η -axis, $l_j(\eta)$ are the Lagrange interpolation polynomials, and $C_{ij}^{(r)}$ are the weighting coefficients for which the explicit recursive formula can be found in Refs (Shu and Richards 1992, Xiang and Yang 2008). The sampling points will be generated by the so-called Gauss-Lobatto-Chebyshev points

$$\eta_i = \frac{1}{2} \left(1 - \cos \left(\frac{i}{N-1} \pi \right) \right), \quad i = 1, 2, \dots, N-2 \quad (25)$$

The two end points are included as $\eta_{N-1} = 0$ and $\eta_N = 1$. Applying the relationships (23) and (24) to Eqs. (10) and (11), a total number of $2N_e \times (N-2)$ equations are obtained

$$\alpha_{1n} \sum_{j=1}^N C_{ij}^{(1)} v_j^{(n)} + \alpha_{2n} \psi_i^{(n)} + \alpha_{3n} \sum_{j=1}^N C_{ij}^{(2)} \psi_j^{(n)} + \ddot{\psi}_i^{(n)} = 0 \quad (26)$$

$$\beta_{1n} v_i^{(n)} + \beta_{2n} \sum_{j=1}^N C_{ij}^{(2)} v_j^{(n)} + \beta_{3n} \sum_{j=1}^N C_{ij}^{(1)} \psi_j^{(n)} + \ddot{v}_i^{(n)} = f_i \quad (27)$$

for $i = 1, 2, \dots, N-2$ and $n = 1, 2, \dots, N_e$. Two dots over a variable denote the second derivative of that variable with respect to time. The continuous conditions (12)-(15), periodic boundary conditions (16)-(19) or boundary conditions (20)-(22) can be changed in a similar way.

For an infinite periodic beam, together with $4(N_e-1)$ continuous conditions, four periodic boundary conditions and $2N_e \times (N-2)$ equations from governing equations (26)-(27), a total number of $2N_e \times N$ equations are obtained. The total number of independent unknown variables $v_i^{(n)}$ and $\psi_i^{(n)}$ is also equal to $2N_e \times N$. Thus, the problem can be solved numerically.

For a finite quasi-periodic beam, comparing with the periodic beam, the only change is to replace the periodic boundary conditions by four specific boundary conditions. For example, substituting the DQM rule (23) and (24) to Eqs. (21) and (22), four boundary conditions for a cantilever beam can be approximated as

$$v_{N-1}^{(1)} = v_0, \psi_{N-1}^{(1)} = \psi_0 \tag{28}$$

at the clamped end, and

$$\gamma_{2N_e} \psi_N^{(N_e)} + \gamma_{3N_e} \sum_{j=1}^N C_{N,j}^{(1)} v_j^{(N_e)} = \bar{Q}_0, \gamma_{1N_e} \sum_{j=1}^N C_{N,j}^{(1)} \psi_j^{(N_e)} = \bar{M}_0 \tag{29}$$

at the free end.

Therefore, we obtained $2N_e \times N$ equations whether an infinite periodic beam or a finite quasi-periodic beam is considered. These equations can be expressed in a matrix form

$$\begin{bmatrix} \mathbf{M}_{dd} & 0 \\ 0 & 0 \end{bmatrix} \begin{pmatrix} \ddot{\boldsymbol{\delta}}_d \\ \ddot{\boldsymbol{\delta}}_b \end{pmatrix} + \begin{bmatrix} \mathbf{K}_{dd} & \mathbf{K}_{db} \\ \mathbf{K}_{bd} & \mathbf{K}_{bb} \end{bmatrix} \begin{pmatrix} \boldsymbol{\delta}_d \\ \boldsymbol{\delta}_b \end{pmatrix} = \begin{pmatrix} \mathbf{p}_d \\ \mathbf{p}_b \end{pmatrix} \tag{30}$$

where $\mathbf{K}_{dd}, \mathbf{K}_{db}, \mathbf{K}_{bd}, \mathbf{K}_{bb}$ and \mathbf{K}_{dd} are coefficient matrices, $\mathbf{p}_d, \mathbf{p}_b$ are two load vectors and

$$\boldsymbol{\delta}_d = (v_1^{(1)}, v_2^{(1)}, \dots, v_{N-2}^{(1)}, \psi_1^{(1)}, \psi_2^{(1)}, \dots, \psi_{N-2}^{(1)}, \dots, v_1^{(N_e)}, v_2^{(N_e)}, \dots, v_{N-2}^{(N_e)}, \psi_1^{(N_e)}, \psi_2^{(N_e)}, \dots, \psi_{N-2}^{(N_e)})^T$$

$$\boldsymbol{\delta}_b = (v_{N-1}^{(1)}, v_N^{(1)}, \psi_{N-1}^{(1)}, \psi_N^{(1)}, v_{N-1}^{(2)}, v_N^{(2)}, \psi_{N-1}^{(2)}, \psi_N^{(2)}, \dots, v_{N-1}^{(N_e)}, v_N^{(N_e)}, \psi_{N-1}^{(N_e)}, \psi_N^{(N_e)})^T$$

Subscripts ‘ d ’ and ‘ b ’ refer to the values at the domain and the boundary grid points, respectively. Eq. (30) can be reduced to the following equation.

$$\mathbf{M}_{dd} \ddot{\boldsymbol{\delta}}_d + \tilde{\mathbf{K}}_{dd} \boldsymbol{\delta}_d = \tilde{\mathbf{p}}_d \tag{31}$$

$$\boldsymbol{\delta}_b = \mathbf{K}_{bb}^{-1} (\mathbf{p}_b - \mathbf{K}_{bd} \boldsymbol{\delta}_d) \tag{32}$$

where $\tilde{\mathbf{K}}_{dd} = \mathbf{K}_{dd} - \mathbf{K}_{db} \mathbf{K}_{bb}^{-1} \mathbf{K}_{bd}$ and $\tilde{\mathbf{p}}_d = \mathbf{p}_d - \mathbf{K}_{db} \mathbf{K}_{bb}^{-1} \mathbf{p}_b$. Eqs. (31)-(32) can be used to solve several subset problems, including the band gap in an infinite periodic beam and the free vibration, harmonic frequency response and transient response of a finite quasi-periodic beam.

For a transient response problem, Eq. (31) can be solved by the Newmark β method, the Wilson θ method, or others (Chopra 2006). In the present work, the Newmark β method is adopted and the parameters for Newmark scheme are chosen as $\alpha = 1/2$ and $\beta = 1/4$.

If a harmonic frequency response analysis is considered, the excitation force $\tilde{\mathbf{p}}_d$ is assumed to be a harmonic time function as $\tilde{\mathbf{p}}_d = \mathbf{p}_0 e^{i\Omega\tau}$ where $\bar{\Omega} = \Omega \sqrt{\rho_0 A_0 / E_0}$ represents the dimensionless

frequency, Ω the imposed circular frequency, \mathbf{p}_0 the force amplitude. The steady-state vibration should be in the form of $\delta_d = \delta_{\max} e^{i\Omega\tau}$ where δ_{\max} is the amplitude of displacement vector. Substituting δ_d and $\tilde{\mathbf{p}}_d$ into Eq. (31), the steady-state solution can be obtained as follows

$$\delta_{\max} = (\tilde{\mathbf{K}}_{dd} - \bar{\Omega}^2 \mathbf{M}_{dd})^{-1} \mathbf{p}_0 \quad (33)$$

For a free vibration problem, neglecting the dynamic load vector $\tilde{\mathbf{p}}_d$, expanding the dynamic vector $\delta_d = \delta_0 e^{i\bar{\omega}\tau}$ where $\bar{\omega} = \omega \sqrt{\rho_0 A_0 / E_0}$ represents the dimensionless frequency, ω the natural circular frequency, and δ_0 the vibration mode shape vector, and then substituting this expansion into Eq. (31), we obtain the following eigenvalue equation

$$(\tilde{\mathbf{K}}_{dd} - \bar{\omega}^2 \mathbf{M}_{dd}) \delta_0 = 0 \quad (34)$$

from which the natural frequencies and associated mode shapes of the beam can be calculated.

Analogously to the above case of free vibration, the eigenvalue equation for an infinite periodic beam can be obtained using the periodic boundary condition instead of the boundary conditions for a finite beam. As indicated in Eqs. (16)-(19), the matrix $\tilde{\mathbf{K}}_{dd}$ is a matrix function of the wave number k , so the eigenvalue equation for an infinite periodic beam can be written as

$$[\tilde{\mathbf{K}}_{dd}(k) - \bar{\omega}^2 \mathbf{M}_{dd}] \delta_0 = 0 \quad (35)$$

The eigenvalue of the Eq. (35) can be determined if the value of k is specified. Though the wave number k is unrestricted, it is only necessary to consider k limited to the first Brillouin zone (Kittel 2005), i.e., $k \in [-1, 1]$. In fact, if we chose a wave number k_0 different from the original k in the first Brillouin zone by a reciprocal lattice vector, for example $k_0 = k + 2n$ where n is an integer, we would have obtained the same set of periodic boundary conditions because $e^{ik_0\pi} = e^{ik\pi}$.

4. Validation study

Before carrying out the dynamic analysis of periodic or quasi-periodic beams, the accuracy and flexibility of the present method are validated through comparisons with existing solutions available in previous studies of homogeneous beams without elastic foundations. Using the differential quadrature method, the band gaps in infinite periodic beams and the dispersion relationship for infinite homogeneous beams were obtained and validated in our previous study (Xiang and Shi 2009). Hence, in present work, we will focus our efforts on the natural frequencies, harmonic frequency response and transient response of the finite periodic beams. The material properties are listed in Table 1. A rectangular cross-section, 0.5 m wide by 0.8 m high, is considered in this

Table 1 Material properties

| Materials | Young's Modulus E (GPa) | Shear modulus G (GPa) | Density ρ (kg/m ³) |
|-----------|------------------------------|----------------------------|--|
| Steel | 210 | 78.95 | 7850 |
| Concrete | 25 | 9.40 | 2300 |

section for all beams.

Based on the Euler-Bernoulli beam theory (EBT), Timoshenko (1937) presented an analytical formula for calculating the natural frequency of finite beams. Huang (1961) obtained the frequency equation for flexural vibrations of finite beams based on Timoshenko beam theory (TBT). Solving these frequency equations, the exact natural frequencies of Timoshenko beams can be obtained easily. Table 2 lists the first three frequencies of common types of concrete beams with length 2 m or 20 m. Our results, either for the slender beam or the short deep beam, are very close to Huang’s analytical solutions (Huang 1961). Table 2 also shows that the results obtained by EBT are larger than present results, especially for a deep beam of which the total length is 2 m. This observation is rational, since the shear deformation is neglected in the Euler-Bernoulli formulations and it makes the beam behavior invalidly stiffer than the reality.

Table 2 Comparison of the first three frequencies of concrete beams with different boundary conditions and length (Hz)

| Boundary condition and mode | Length = 20 m | | | Length = 2 m | | | |
|-----------------------------|------------------|------------------|---------|------------------|------------------|-----------|-----------|
| | EBT ^a | TBT ^b | Present | EBT ^a | TBT ^b | Present | |
| CF | 1 | 1.0650 | 1.0638 | 1.0638 | 106.5045 | 95.1900 | 95.1900 |
| | 2 | 6.6750 | 6.6157 | 6.6157 | 667.5002 | 399.1341 | 399.1341 |
| | 3 | 18.6921 | 18.3016 | 18.3021 | 1869.2080 | 853.0115 | 853.0120 |
| SS | 1 | 2.9900 | 2.9818 | 2.9818 | 298.9957 | 242.9095 | 242.9095 |
| | 2 | 11.9598 | 11.8305 | 11.8306 | 1195.9829 | 702.1181 | 702.1181 |
| | 3 | 26.9096 | 26.2709 | 26.2713 | 2690.9616 | 1193.5004 | 1193.5068 |
| CC | 1 | 6.7778 | 6.7023 | 6.7023 | 677.7781 | 379.2692 | 379.2692 |
| | 2 | 18.6826 | 18.2131 | 18.2131 | 1868.2563 | 763.2160 | 763.2160 |
| | 3 | 36.6298 | 35.0501 | 35.0500 | 3662.9814 | 1217.4782 | 1217.4782 |

^aTimoshenko 1937;

^bHuang 1961.

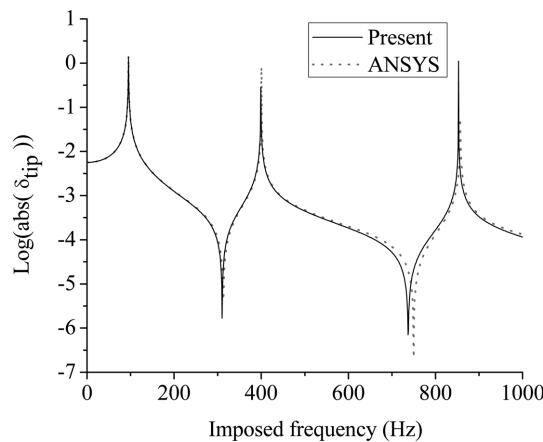


Fig. 2 Frequency response of a homogeneous concrete cantilever beam

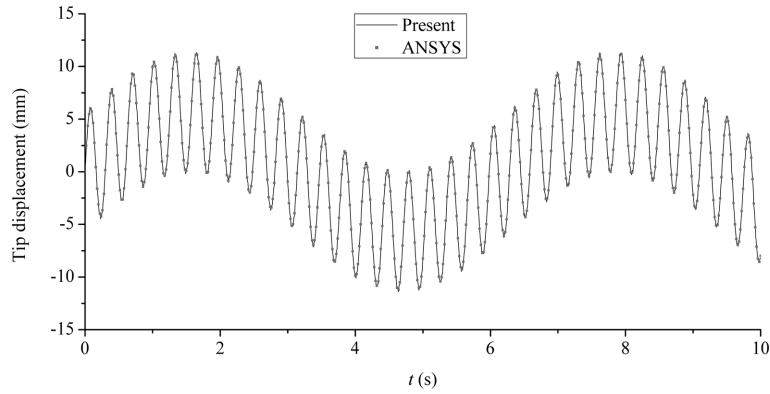


Fig. 3 Tip displacement history of a homogeneous concrete cantilever beam subject to a tip force $F(t) = 1000(\sin t + \sin 20t)$ kN

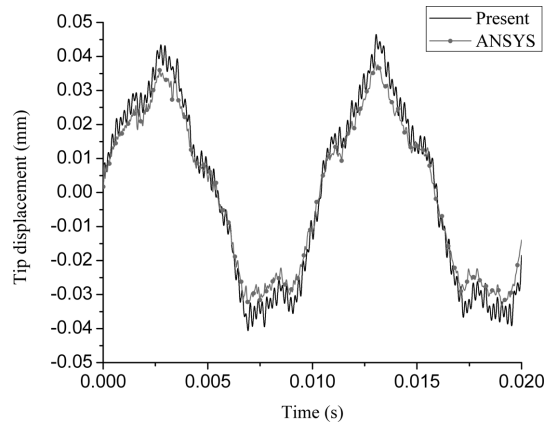


Fig. 4 Tip displacement history of a homogeneous concrete cantilever beam subject to an impact force at the free end

Fig. 2 depicts the frequency response of tip deflections δ_{tip} of a concrete cantilever beam with length 2 m subjected to a harmonic load at the free end. The load amplitude is 1000 kN. A finite element model was built in ANSYS using the BEAM188 element which is based on Timoshenko beam theory. In the present example, linear shape functions are used. This element produces a stiffer response as is evident in Fig. 2 by the slight offset to the right.

Fig. 3 shows the tip deflection time history by the present method and the ANSYS model for the cantilever beam subjected to a harmonic force $F(t) = 1000(\sin t + \sin 20t)$ kN at the free end. When an impact load is applied at the free end, the transient tip displacement responses are shown in Fig. 4. The impact load is assumed as

$$F(t) = \begin{cases} 1000 \text{ kN}, & 0 \leq t \leq 10^{-5} \text{ s} \\ 0, & t > 10^{-5} \text{ s} \end{cases}$$

The integration time step (ITS) should be small enough to resolve the motion (response) of the beam and to “follow” the loading function. The ITS is specified as 0.01 s for the harmonic load

case and 10^{-5} s for the impact load case. The results for both the harmonic load and the impact load, match well with the FEM results obtained by ANSYS.

5. Numerical results

In this section, we will investigate the band gap in periodic beams on a Pasternak foundation and study the frequency response and the transient response of the quasi-periodic beams. As shown in Fig. 1, material A is concrete and material B is steel. Unless otherwise stated, the shear foundation modulus $K_G = 3000$ kN and the Winker modulus $K_w = 6 \times 10^8$ N/m² are considered for both sections. The total length of substructure AB is $a = a_1 + a_2 = 2$ m. The length of beam section A is equal to that of B, i.e., $a_1 = a_2$. In order to show the effect of geometrical parameters on flexural vibration, two cases, I and II, are considered. For the case I, the cross sections of both sections A and B are rectangle 0.5 m wide and 0.8 m deep. For the case II, the sections A and B are the rectangle and a wide flanged H-section, respectively. The geometrical parameters of the wide flanged H section are $I = 3.5914 \times 10^{-3}$ m⁴, $A = 0.0314$ m² and the shear correction factor $k_s = 0.3564$ (Cowper 1966). In what follows, the dimensionless frequency is defined as $\bar{\omega} = \omega \sqrt{\rho_0 A_0 / E_0}$, where ρ_0 , A_0 and E_0 are the density, the cross-section area and the modulus of elasticity of the beam section A, respectively. The number of sampling points is denoted by N . Experience with the analysis method shows good convergence when $N \geq 10$, thus the present analysis utilizes $N = 13$.

5.1 Band gap in infinite periodic beams

The band structures of the infinite beams for the case I and the case II are depicted in Figs. 5(a) and 5(b), respectively. Two frequency ban gaps are found in both cases, which are shaded. For the case I, the first band gap is very narrow (0.2835-0.3114). The second band gap starts from 0.7313 and ends at 1.0402. On the other hand, by comparison with the case I, a wider first band gap (0.3077-0.5269) is obtained for the case II. However, the second band gap for this case is relative narrow (0.7841-1.0413). After performing many numerical tests, we found that the greater the

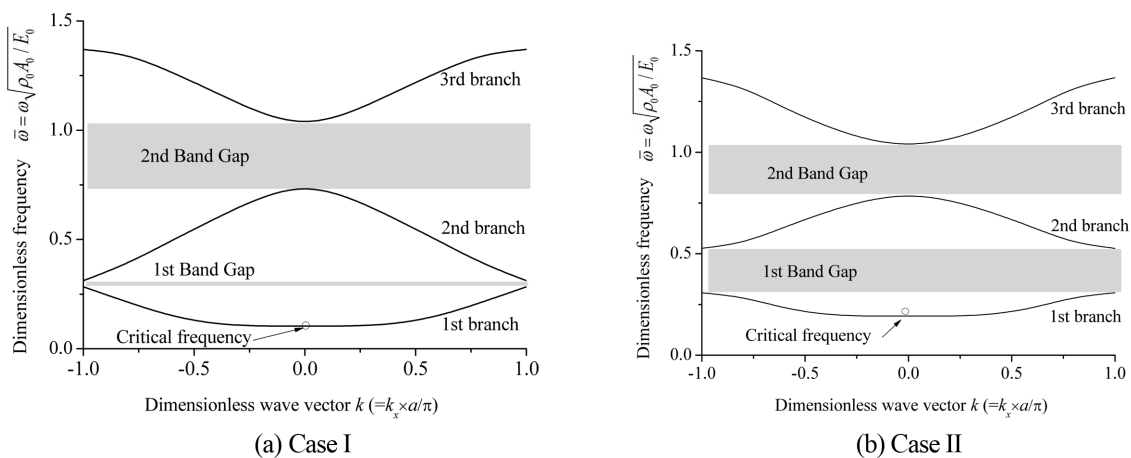


Fig. 5 Band structures of two cases of infinite periodic beams on elastic foundation

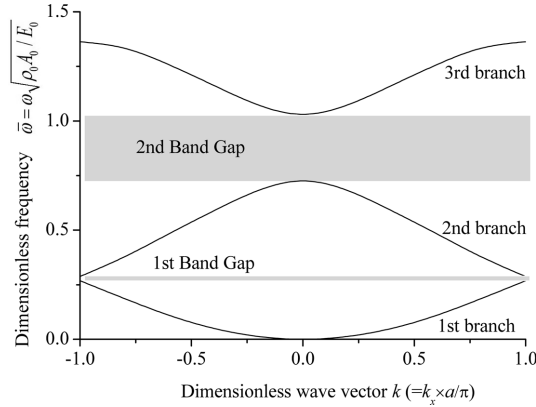


Fig. 6 Band structures of an infinite periodic beam without elastic foundation

difference in the value of $(c_1/a)^2 + (c_2/r)^2$ between sections A and B, the wider the first band gaps. Herein, $c_1 = \sqrt{E/\rho}$, $c_2 = \sqrt{k_s G/\rho}$ and $r = \sqrt{I/A}$ are the velocity of bending wave, the velocity of shear wave and the radius of gyration, respectively. This is similar to the dynamic behavioral characteristics of composite materials observed in previous works. For example, Kafesaki and Economou (1995) studied the band structures of acoustic waves in composites. They observed that the higher the velocity ratio between the components of the composite, the more favorable the condition for gaps. However, this is only a qualitative conclusion without a strict derivation.

For comparison purpose, the band structure of the beam without elastic foundation is also plotted for the case I in Fig. 6. We can find that the frequency in the first branch is zero at $k = 0$. However, as shown in Fig. 5, no curve appears in the band structure when the frequency is lower than the critical frequency that is defined as the frequency in the first branch when $k = 0$. The dimensionless critical frequencies for the case I and the case II are 0.1041 and 0.1932, respectively. Both of them are positive numbers instead of zero. This phenomenon can be explained by the well-known Rayleigh’s theorem, which may be stated as follows (Wittrick and Williams 1971).

If one constraint is imposed upon a linearly elastic structure, the natural frequencies of the constrained structure remains unchanged or increase. If the unconstrained structure has no coincident natural frequencies, and if none of its natural modes has a node coinciding with the constraint, then the natural frequencies of the constrained structure will increase.

The word constraint may be understood to imply the addition of a simple spring, attached to the structure at an arbitrary point and in an arbitrary direction. In the present example, the foundation, which is severed as a continuous constraint, leads to a shift of the critical frequency from zero to a positive number. In order to get a formula to calculate the critical frequency, we consider a homogenous beam at first. It is assumed that the beam undergoes harmonic wave $(w, \psi) = (W, \Phi)e^{i(k_x x - \omega t)}$ where W and Φ are the amplitude of transverse deflection and the amplitude of the bending slope, respectively. Substituting this expression into Eqs. (1) and (2), and letting the wave number $k_x = 0$, one can get two solutions as follows

$$\omega_1 = \sqrt{\frac{K_w}{\rho A}}, \quad \omega_2 = \sqrt{\frac{k_s GA}{\rho I}} \tag{36}$$

which the frequencies ω_1 and ω_2 are related to the bending and the shear mode, respectively. Usually, $\omega_2 > \omega_1$ unless the Winkler foundation modulus is very large. Therefore, the frequencies ω_1

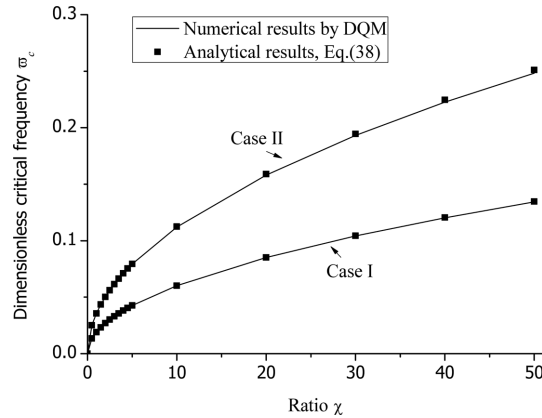


Fig. 7 Critical frequencies v.s. Winker foundation modulus

is the critical frequency for the homogenous beam on a Pasternak foundation. It is noted that, for ω_1 , the motion is associated to a long-wave with transverse deflection without shear, i.e., a translational motion $(w, \psi) = (W, 0)e^{-i\omega t}$. The continuous system degenerates to a single degree system. Thus, the physical meaning of the critical frequency can be explained through the vibration of a unit length of the beam. The total mass of the unit length is ρA and the transverse stiffness is K_w , so the circular frequency is $\omega_1 = \sqrt{K_w/\rho A}$ for the single degree of freedom system. In this manner, similarly, we can also get a formula to calculate the critical frequency for periodic beams through the vibration of a unit cell. The total mass of a cell of the periodic beam, as shown in Fig. 1, is $\rho^{(1)}A^{(1)}a_1 + \rho^{(2)}A^{(2)}a_2$. When the transverse deflection is a unit, the total ground reaction force (or stiffness) is $K_w^{(1)}a_1 + K_w^{(2)}a_2$, and then the critical frequency for periodic beams can be expressed as

$$\omega_c = \sqrt{\frac{K_w^{(1)}a_1 + K_w^{(2)}a_2}{\rho^{(1)}A^{(1)}a_1 + \rho^{(2)}A^{(2)}a_2}} \tag{37}$$

or in dimensionless form as

$$\bar{\omega}_c = \sqrt{\frac{(K_w^{(1)}a_1 + K_w^{(2)}a_2)\rho_0 A_0}{E_0(\rho^{(1)}A^{(1)}a_1 + \rho^{(2)}A^{(2)}a_2)}} \tag{38}$$

where the subscripts “c” stands for critical frequency. The dimensionless critical frequencies of periodic beams with different Winkler modulus are plotted in Fig. 7. The ratio $\chi = K_w/K_{w0}$ and $K_{w0} = 2 \times 10^7 \text{ N/m}^2$. Excellent agreement is observed between the results obtained by DQM and the analytical results by Eq. (38). Moreover, as mentioned above, the critical frequency is zero if a periodic beam without foundation is considered. As a special case, this result can be calculated from Eq. (38), i.e., $K_w^{(1)} = K_w^{(2)} = 0$ and then $\bar{\omega}_c = 0$.

5.2 Harmonic frequency response

To illustrate the vibration attenuation in periodic beams, a finite quasi-periodic cantilever beam was examined. The cantilever beam is composed of eight sections A and eight sanctions B and

subjected to a harmonic dynamic support displacement $w_0(\tau)$ at the clamed end. The cross-section is the same as that of the case II. The harmonic dynamic support displacement with amplitude δ_0 is taken as $w_0(\tau) = \delta_0 \sin(\bar{\Omega}, \tau)$ where $\bar{\Omega}$ is the imposed frequency. The tip displacement amplitude δ_{tip} at the free end is calculated by the present method. Instead of the band structure for an infinite structure, the transmitting frequency response function (FRF) is a primary representation of the dynamic property for the finite periodic beam. The FRF is defined as $20\log(\delta_{tip}/\delta_0)$. Note that if the displacement δ_0 and the tip displacement δ_{tip} are the same then the value of FRF will be 0. Therefore, a negative number in FRF indicates a very effective reduction. It is found that the tip displacement is strongly reduced when the frequency of support excitation is located within the band gaps given in Section 5.1. Note that the dimensionless critical frequency $\bar{\omega}_c$ is 0.1932 in this example. While $\bar{\Omega} < \bar{\omega}_c$, the vibration is also attenuated but in a different way. The essential difference of the two types of attenuations is that the former is caused by the periodicity of materials and the latter is due to the exiting of foundation.

In order to facilitate a direct comparison of the vibration characteristics, the tip displacements of a homogeneous uniform concrete beam of the same length and loading input as the periodic beam discussed above are also calculated. The dimensionless critical frequency for the concrete beam is 0.1549. The results are shown in Fig. 8(b). It is found that homogeneous beams do not exhibit vibration attenuation while $\bar{\Omega} > \bar{\omega}_c$, because there are no band gaps in homogeneous beams as stated previously. This research also produced results for a steel beam. Although both types of homogeneous beams have been analyzed, only the results for the concrete beam are presented, as the results for these two types are quite similar.

As shown in Fig. 8(a), the minimum value of frequency response function (MFRF) indicates the maximum attenuation. It is a further interesting to study the effect of the foundation on MFRF. The shear foundation modulus is kept constant but the Winker foundation modulus is varied such that the ratio $\chi = K_w/K_{w0}$ changes from 0 to 50. On contrast, the Winker foundation modulus remains unchanged but the shear foundation modulus is changed from 0 to $50K_{G0}$ ($K_G = \lambda K_{G0}, \lambda \in [0, 50]$). Figs. 9(a) and 9(b) compare the effect of K_w and K_G on MFRF when the imposed frequency falls into the first band gap and the second band gaps, respectively. Herein, $K_{w0} = 2 \times 10^7 \text{ N/m}^2$ and $K_{G0} = 3 \times 10^6 \text{ N}$. It is found that the MFRF is decreased in both band gaps as the increasing of K_w ,

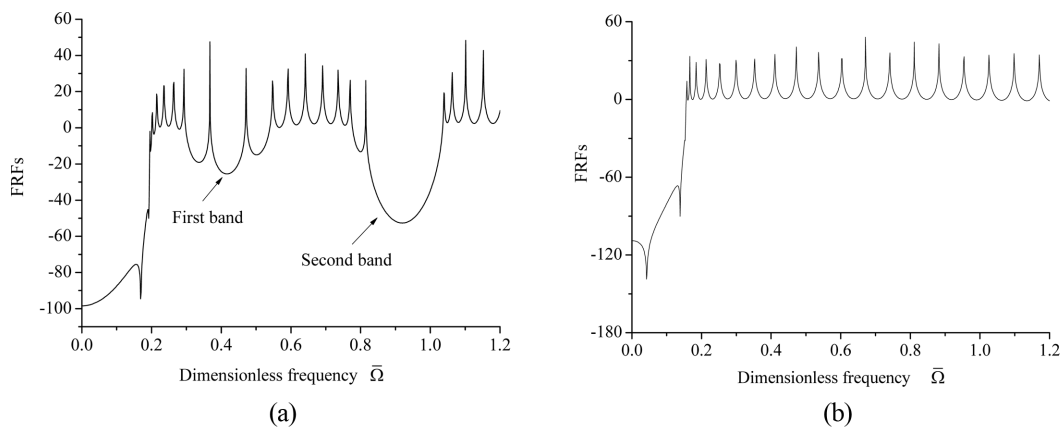


Fig. 8 Frequency response of the tip displacement of finite cantilever beams (a) periodic beam and (b) homogenous beam. $\delta_0 = 1 \text{ mm}$

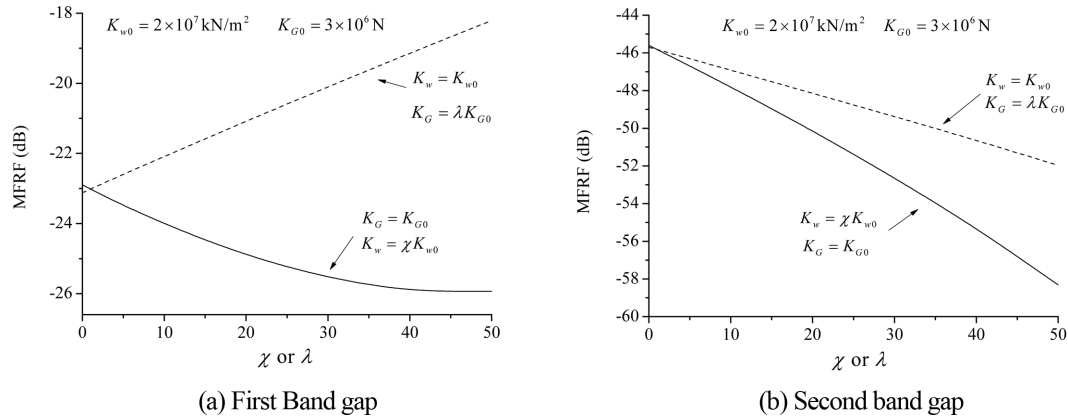


Fig. 9 Effect of elastic foundation on MFRF in the first two band gaps

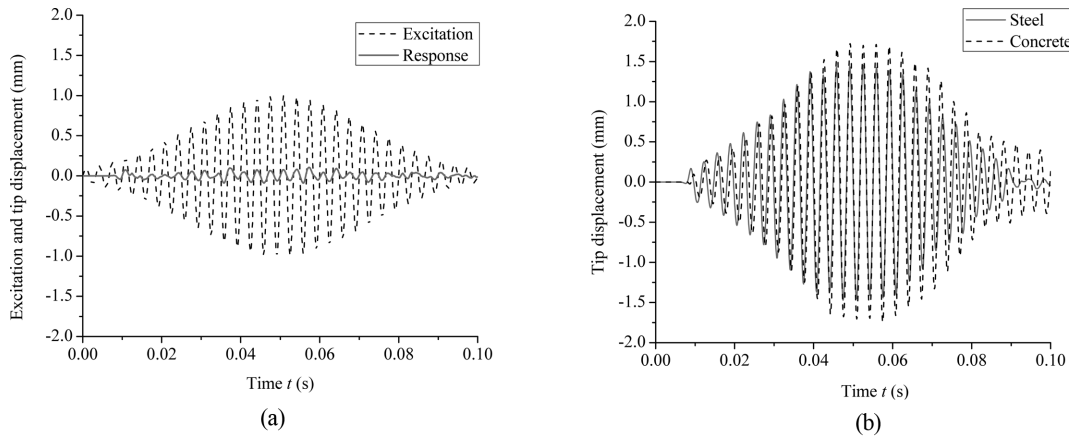


Fig. 10 Tip displacements history: (a) response of a periodic beam and the support excitation and (b) response of homogenous beams

whereas the MFRF is increased in the first band and, however, decreased in the second band when the shear modulus K_G is changed from 0 to $50K_{G0}$.

5.3 Transient response

As an example, the quasi-periodic cantilever described in Section 5.2 is considered but without elastic foundation. A dynamic support displacement is applied at the fixed end. The support displacement is assumed to be a sinus function damped by a symmetric exponential function: $w_0(t) = e^{-1000(t-0.05)^2} \sin(2\pi \cdot 300 \cdot t)$ mm, which is plotted in Fig. 10(a). Note that the excitation is similar to an earthquake motion and the frequency 300 Hz falls into the band gap (214.5 Hz-391.9 Hz). The tip displacements of the quasi-periodic beam are also illustrated in Fig. 10(a). The ITS in this example is 0.0001 s. Again, vibration attenuation is observed. However, the dynamic response at the free end of a homogeneous concrete (or steel) cantilever is enlarged as shown in Fig. 10(b).

5.4 Effect of foundations on band gaps

In what follows, numerical studies are presented to highlight the effect of elastic foundations on the first band gap. The ratio $\chi = K_w/K_{w0}$ and $K_{w0} = 2 \times 10^7$ N/m². The shear modulus K_G of the foundation is taken as a constant 3000 kN because both the start frequency and width of the first band gap in periodic beams are much less sensitive to the changes of shear modulus of the foundation.

For both cases, I and II, three types of beams with different cell lengths, $a = 2$ m, 10 m, and 20 m, were analyzed. Figs. 11(a) and 11(b) show the effect of the Winker modulus K_w on the band width of the first band gap. Figs. 12(a) and 12(b) show the effect of Winkler modulus on start frequency (lower bound frequency). Both figures are plotted in the domain of χ from 0 to 50. For the beam of short cell ($a = 2$ m), both the band width and start frequency increase approximately linearly. For the beams of longer cell ($a = 10$ m, $a = 20$ m), the gap bandwidth shows an initial rapid increase or sensitivity to increasing Winkler modulus but then levels off or begins to decrease.

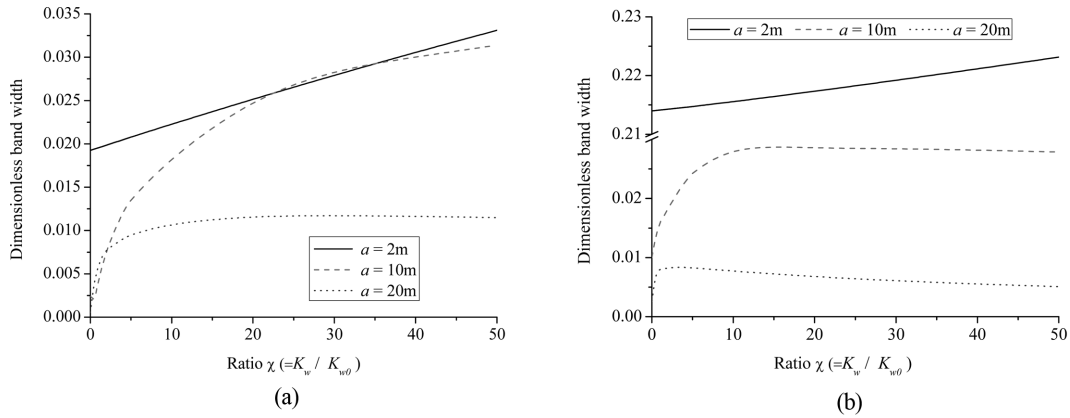


Fig. 11 Effect of elastic foundation on the band width of the first band gap (a) uniform cross-section and (b) variable cross section (section A – rectangle and section B – H section)

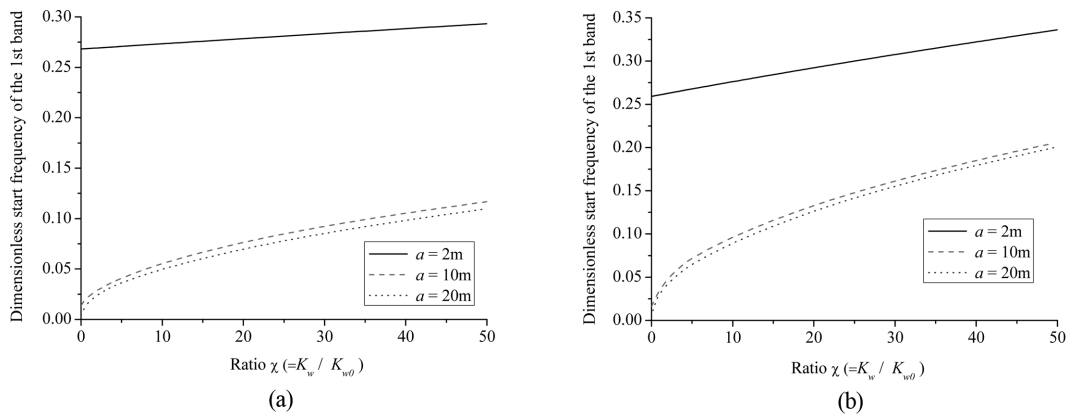


Fig. 12 Effect of elastic foundation on start frequencies of the first band gap: (a) uniform cross-section and (b) variable cross section (section A – rectangle and section B – H section)

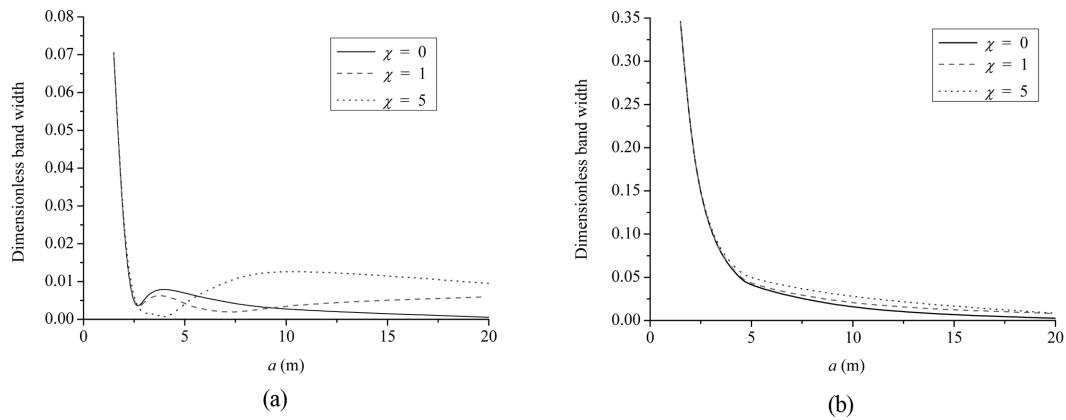


Fig. 13 Effect of the length a on the band width of the first band gap: (a) uniform cross-section and (b) variable cross section (section A – rectangle and section B – H section)

Table 3 Dimensionless start frequency of the first band gap in periodic composite beams

| a (m) | Uniform cross section | | | Variable cross section | | |
|---------|-----------------------|----------------|-----------------|------------------------|----------------|-----------------|
| | $K_w = 0$ | $K_w = K_{w0}$ | $K_w = 5K_{w0}$ | $K_w = 0$ | $K_w = K_{w0}$ | $K_w = 5K_{w0}$ |
| 1.5 | 0.3980 | 0.3983 | 0.3998 | 0.3841 | 0.3853 | 0.3901 |
| 2 | 0.2682 | 0.2687 | 0.2708 | 0.2592 | 0.2609 | 0.2679 |
| 2.5 | 0.1922 | 0.1929 | 0.1958 | 0.1860 | 0.1885 | 0.1979 |
| 3 | 0.1381 | 0.1400 | 0.1474 | 0.1394 | 0.1427 | 0.1549 |
| 3.5 | 0.1035 | 0.1060 | 0.1157 | 0.1080 | 0.1122 | 0.1274 |
| 4 | 0.0803 | 0.0836 | 0.0958 | 0.0859 | 0.0911 | 0.1093 |
| 4.5 | 0.0641 | 0.0683 | 0.0810 | 0.0699 | 0.0760 | 0.0971 |
| 5 | 0.0523 | 0.0574 | 0.0702 | 0.0578 | 0.0652 | 0.0889 |
| 10 | 0.0136 | 0.0233 | 0.0409 | 0.0159 | 0.0341 | 0.0689 |
| 20 | 0.0036 | 0.0172 | 0.0364 | 0.0043 | 0.0300 | 0.0650 |

The gap start frequency for the long beams also shows an initial rapid increase with increasing Winkler modulus ratio, but then increases only constantly. Obviously, the Winkler foundation modulus increment enhances the beam stiffness and thus increases the start frequency of band gaps.

Figs. 13(a) and 13(b) show the effect of length a on the band width of the first band gap in periodic beams for the two case I and II with $\chi = 0, 1$ and 5 . A significant effect of the length a is observed, especially as the value of a gets smaller and smaller. A regular trend is not observable for bandwidth for either type of beams with long length values of a . However, it is noted that as the length a becomes larger and larger, the beam becomes a beam with two semi-infinite homogeneous beam sections. As previously mentioned, homogeneous beams do not exhibit frequency band gaps. The band width should tend to zero as $a \rightarrow +\infty$. To explain this more clearly, Table 3 lists the dimensionless start frequencies of the first band gap with different length a and Winkler foundation modulus ($K_w = 0, K_{w0}$ and $5K_{w0}$). This research has shown that the start frequencies decrease as the length a increases. Furthermore, the effect of Winkler foundation modulus on the start frequencies

becomes more and more significant as the length a increase. The start frequencies with different K_w are almost equal when $a = 1.5$ m. However, the start frequency for $K_w = 5K_{w0}$ is almost ten times of that for $K_w = 0$ when $a = 20$ m. Therefore, a periodic beam can be designed to isolate vibrations for a specified or desired frequency.

6. Conclusions

Based on the Timoshenko beam theory, the differential quadrature method was introduced to analyze the free vibration, frequency response, time history response and frequency band gaps of periodic and quasi-periodic beams on Pasternak foundation. The following conclusions may be drawn from the present analysis:

- 1) Vibration attenuation for exciting frequency located at band gaps was observed, which can form the basis of new techniques for the vibration isolation of structures.
- 2) The so-called critical frequency is found because of the foundation. Theory analysis shows that the critical frequency is highly dependent on the Winkler foundation modulus K_w instead of the shear foundation modulus K_G .
- 3) The effect of foundation and the cell length a on band gaps in periodic beams is non-negligible. For beams with shorter cell, the band width decreases dramatically as the cell length increases, which means the cell length plays more important role on the band gaps. On the other side, the larger value of length a , the effect of foundation on the band gaps are more sensitive. Therefore, we can adjust the cell length to get a appreciate band gap for a certain foundation or soil condition.

Although we only demonstrate the DQM for periodic beams, it is firmly believed that the method can be extended to two or three dimensional periodic structures. Further effort can be done on higher dimensional periodic structures and their applications in, for example, civil engineering.

Acknowledgements

This work is supported by the National Natural Science Foundation of China (50808012 and 90715006).

References

- Bert, C.W. and Malik, M. (1996), "Differential quadrature method in computational mechanics: a review", *Appl. Mech. Rev.*, **49**(1), 1-28.
- Celep, Z. and Demir, F. (2007), "Symmetrically loaded beam on a two-parameter tensionless foundation", *Struct. Eng. Mech.*, **27**(5), 555-574.
- Chopra, A.K. (2006), *Dynamics of Structures - Theory and Applications to Earthquake Engineering*, 3rd edition, Prentice Hall, New Jersey.
- Coskun, I. (2010), "Dynamic contact response of a finite beam on a tensionless Pasternak foundation under symmetric and asymmetric loading", *Struct. Eng. Mech.*, **34**(3), 319-334.
- Cowper, G.R. (1966), "The shear coefficient in Timoshenko's beam theory", *J. Appl. Mech.*, **33**, 335-340.
- Fan, H.L., Meng, F.H. and Yang, W. (2007), "Sandwich panels with Kagome lattice cores reinforced by carbon

- fibers”, *Compos. Struct.*, **81**(4), 533-539.
- Faulkner, M.G. and Hong, D.P. (1985), “Free vibrations of a mono-coupled periodic system”, *J. Sound Vib.*, **99**(1), 29-42.
- Hsieh, P.F., Wu, T.T. and Sun, J.H. (2006), “Three-dimensional phononic band gap calculations using the FDTD method and a PC cluster system”, *IEEE T. Ultrason Ferr.*, **53**(1), 148-158.
- Huang, T.C. (1961), “The effect of rotatory inertia and of shear deformation on the frequency and normal mode equations of uniform beams with simple end conditions”, *J. Appl. Mech.*, **28**(4), 579-584.
- Jia, G.F. and Shi, Z.F. (2010), “A new seismic isolation system and its feasibility study”, *Earthq. Eng. Eng. Vib.*, **9**(1), 75-82.
- Kafesaki, M. and Economou, E.N. (1995), “Interpretation of the band structure results for elastic and acoustic waves by analogy with the LCAO approach”, *Phys. Rev. B*, **52**(18), 13317-13331.
- Khelif, A., Aoubiza, B., Mohammadi, S., Adibi, A. and Laude, V. (2006), “Complete band gaps in two-dimensional phononic crystal slabs”, *Phys. Rev. E*, **74**(4), 046610-1-5.
- Kittel, C. (2005), *Introduction to Solid State Physics*, 8th edition, John Wiley & Son, New York.
- Kushwaha, M.S. (1996), “Classical band structure of periodic elastic composites”, *Int. J. Mod. Phys. B*, **10**(9), 977-1094.
- Kushwaha, M.S., Halevi, P., Dobrzynski, L. and Djafarirouhani, B. (1993), “Acoustic band structure of periodic elastic composites”, *Phys. Rev. Lett.*, **71**(13), 2022-2025.
- Lee, S.Y. and Ke, H.Y. (1992), “Flexural wave propagation in an elastic beam with periodic structure”, *J. Appl. Mech.*, **59**(2), S189-S196.
- Lin, Y.K., Zhang, R. and Yong, Y. (1990), “Multiply supported pipeline under seismic wave excitations”, *J. Eng. Mech.-ASCE*, **116**(5), 1094-1108.
- Mead, D.J. (1986), “A new method of analyzing wave propagation in periodic structures - applications to periodic Timoshenko beams and stiffened plates”, *J. Sound Vib.*, **104**(1), 9-27.
- Mead, D.J. (1996), “Wave propagation in continuous periodic structures: Research contributions from Southampton, 1964-1995”, *J. Sound Vib.*, **190**(3), 495-524.
- Pany, C., Parthan, S. and Mukhopadhyay, M. (2003), “Wave propagation in orthogonally supported periodic curved panels”, *J. Eng. Mech.-ASCE*, **129**(3), 342-349.
- Sainidou, R., Stefanou, N., Psarobas, I.E. and Modinos, A. (2005), “A layer-multiple-scattering method for phononic crystals and hetero structures of such”, *Comput. Phys. Commun.*, **166**(3), 197-240.
- Shu, C. and Richards, B.E. (1992), “Application of generalized differential quadrature to solve 2-dimensional incompressible Navier-Stokes equations”, *Int. J. Numer. Meth. Fluids*, **15**(7), 791-798.
- Timoshenko, S. (1937), *Vibration Problems in Engineering*, 2nd edition, D. Van Nostrand, New York.
- Wang, C.M., Lam, K.Y. and He, X.Q. (1998), “Exact solutions for Timoshenko beams on elastic foundations using Green’s functions”, *Mech. Struct. Mach.*, **26**(1), 101-113.
- Wang, G., Wen, J.H., Liu, Y.Z. and Wen, X.S. (2004), “Lumped-mass method for the study of band structure in two-dimensional phononic crystals”, *Phys. Rev. B*, **69**(18), 184302-1-6.
- Wittrick, W.H. and Williams, F.W. (1971), “General algorithm for computing natural frequencies of elastic structures”, *Q. J. Mech. Appl. Math.*, **24**(3), 263-284.
- Xiang, H.J. and Shi, Z.F. (2009), “Analysis of flexural vibration band gaps in periodic beams using differential quadrature method”, *Comput. Struct.*, **87**(23-24), 1559-1566.
- Xiang, H.J. and Yang, J. (2008), “Free and forced vibration of a laminated FGM Timoshenko beam of variable thickness under heat conduction”, *Compos. Pt. B-Eng.*, **39**(2), 292-303.
- Yao, Z.J., Yu, G.L., Wang, Y.S. and Shi, Z.F. (2009), “Propagation of bending waves in phononic crystal thin plates with a point defect”, *Int. J. Solids Struct.*, **46**(13), 2571-2576.
- Yu, D.L., Wen, J.H., Zhao, H.G., Liu, Y.Z. and Wen, X.S. (2008), “Vibration reduction by using the idea of phononic crystals in a pipe-conveying fluid”, *J. Sound Vib.*, **318**(1-2), 193-205.
- Zhaohua, F. and Cook, R.D. (1983), “Beam elements on two-parameter elastic foundations”, *J. Eng. Mech.-ASCE*, **109**(6), 1390-1402.

Appendix A

$$\alpha_{1n} = -k_s^{(n)} \frac{\rho_0 G^{(n)} l_0}{\rho^{(n)} E_0 l_n} \frac{A^{(n)} A_0}{I^{(n)}}, \quad \alpha_{2n} = -\alpha_{1n} \frac{l_n}{l_0}, \quad \alpha_{3n} = -\frac{E^{(n)} \rho_0}{E_0 \rho^{(n)}} \frac{A_0}{l_n^2}$$

$$\beta_{1n} = \frac{\rho_0 A_0 K_w^{(n)}}{\rho^{(n)} A^{(n)} E_0}, \quad \beta_{2n} = -\frac{\rho_0 A_0}{\rho^{(n)} l_n^2} \left(\frac{K_G^{(n)}}{E_0 A^{(n)}} + k_s^{(n)} \frac{G^{(n)}}{E_0} \right), \quad \beta_{3n} = k_s^{(n)} \frac{\rho_0 A_0 G^{(n)}}{\rho^{(n)} l_0 l_n E_0}$$

$$\gamma_{1n} = -\frac{E^{(n)} I^{(n)} l_0}{E_0 I_0 l_n}, \quad \gamma_{2n} = -k_s^{(n)} \frac{G^{(n)} A^{(n)}}{G_0 A_0}, \quad \gamma_{3n} = \frac{[k_s^{(n)} G^{(n)} A^{(n)} + K_G^{(n)}] l_0}{G_0 A_0 l_n}$$